Soft Matter

PAPER

View Article Online
View Journal | View Issue

Cite this: *Soft Matter*, 2021, **17**, 3775

Designing responsive dressings for inflammatory skin disorders; encapsulating antioxidant nanoparticles into biocompatible electrospun fibres†

Charles Brooker,[a] Richard d'Arcy,[b]* Elisa Mele[a] and Helen Willcock[a]*

Received 8th November 2020,
Accepted 19th January 2021

DOI: 10.1039/d0sm01987a

rsc.li/soft-matter-journal

Inflammatory skin disorders are highly prevalent and current treatments are marred by side-effects. Here, we have designed anti-inflammatory fibrous sheets with the potential to treat low exudate inflammatory skin disorders such as psoriasis or atopic dermatitis. Antioxidant and anti-inflammatory nanoparticles composed of crosslinked poly(propylene sulfide) (PPS) were encapsulated in poly(ethylene oxide) (PEO) fibres *via* electrospinning from an aqueous suspension. The loading of nanoparticles did not adversely effect the homogenous nature of the electrospun fibres; furthermore, nanoparticles retained their morphology, size and anti-inflammatory character after electrospinning. The PPS-nanoparticle-loaded nanofibres were found to be highly cytocompatible when tested on human dermal fibroblasts. These findings suggest they have significant potential to topically treat inflamed tissues that are characterized by high reactive oxygen species (ROS) levels.

1 Introduction

Atopic dermatitis/eczema, psoriasis and seborrheic dermatitis are prevalent inflammatory skin disorders which in the U.S. affect approximately 35.4 million Americans.[1–3] Besides the physical traits associated to these disorders such as skin flaking, rashes/erythema and potentially (psoriatic) arthritis, they also carry a significant psychological toll on the sufferers.[4] Current treatments often rely on antimicrobial and anti-inflammatory therapies. Steroids are a common choice of anti-inflammatory but are also associated with a plethora of serious side-effects and other related disorders such as Cushing's syndrome.[5]

For topical administration, creams and emollients are often used for small molecular drugs, but do not offer the same degree of control in drug release rate with respect to other more advanced delivery modalities. Electrospun fibres represent a more advanced approach to spatially controlled topical drug delivery, allowing precise control over application area and drug release rate through degradation/adsorption of drug-loaded fibres. Electrospun fibres are formed *via* a process called electrospinning, a technique that allows the production of fibrous sheets with tuneable diameters, typically ranging from a few micrometres[6] down to one nanometre.[7] Of note, Restrata®, an electrospun scaffold composed of a poly(lactic-*co*-glycolic acid) (PLGA)–polydioxanone blend, was recently FDA approved for topical wound healing applications, highlighting the translatability of electrospun scaffolds.[8]

Electrospinning also permits the encapsulation of diverse payloads within the polymeric fibre matrix, ranging from small drug molecules[9] to proteins[10] and more recently to nanoparticles.[11] In a recent example of the latter, organic PLGA-nanoparticles were loaded with a therapeutic agent and then electrospun with poly(ethylene oxide) (PEO) and a second drug. This system allowed for a fast release of the second drug from the PEO fibre matrix, but a more sustained drug release of the first drug from the PLGA-nanoparticles,[12] thus permitting the modulation of both early and later stages of wound healing separately.

It should be noted though that degradation products of PLGA are acidic and somewhat inflammatory in their own right;[13] recent studies comparing polysulfides and PLGA found that polysulfides compared favourably for sustained release applications in a mouse model of traumatic optic neuropathy, and in fact displayed inherent anti-inflammatory properties, even without payload. Differently to the polysulfide, PLGA was inflammatory and exacerbated neuropathy.[13] These disparate outcomes are likely due to polysulfides, such as poly(propylene sulfide) (PPS), being oxidation-responsive biomaterials that are

[a] *Materials Department, Loughborough University, Epinal Way, Loughborough, LE11 3TU, UK. E-mail: h.willcock2@lboro.ac.uk*
[b] *Department of Biomedical Engineering, Vanderbilt University, Nashville, TN 37235, USA. E-mail: richard.darcy@vanderbilt.edu*

† Electronic supplementary information (ESI) available. See DOI: 10.1039/d0sm01987a

able to effectively scavenge reactive oxygen species (ROS)[14] in a manner that is biomimetic to that of methionine.[15] Sulfides (also known as thioethers) are composed of sulfur in its lowest oxidation state(II), which when exposed to ROS, *e.g.* hydrogen peroxide, oxidizes them to higher polarity sulfoxides (sulfur IV), while stronger oxidants, *e.g.* hypochlorite, lead to formation of sulfones (sulfur VI); the latter of which is often accompanied by depolymerization/chain fragmentation.[16,17] In the case of PPS, the transition from sulfide to sulfoxide/sulfone results in a hydrophobic-to-hydrophilic polarity transition which can be exploited for *e.g.* micelle, polymersome or nanoparticle destabilization/solubilization and site-specific release of encapsulated drug cargos.[18] This makes them attractive for targeting inflammatory pathologies characterized by markedly increased levels of ROS,[16] including wounds and inflammatory skin disorders.[19–21]

Since ROS are effectively scavenged by polysulfides, this also makes them potent antioxidants. As a result, more recent studies have evaluated polysulfides as stand-alone pharmacologically-active ROS-sponges, rather than solely as oxidation-responsive drug-carriers.[15] These 'ROS-sponges' demonstrate a strong capability to therapeutically reduce inflammation in traumatic brain injuries,[22] stroke,[23] ischemia and osteoarthritis;[24] while injectable poly(ethylene glycol) (PEG)–PPS hydrogels were able to safely harbour neuronal progenitor stem cells when co-injected into the brain of a mouse.[25] In a separate hybrid antioxidant-drug delivery approach, polysulfide micelles were able to both therapeutically scavenge ROS and release rapamycin, with both of these events contributing in a synergistic manner to inhibit osteoclastogenesis.[26]

Unlike conventional small-molecular drugs, sustained release of polysulfides, particularly for topical applications, is non-trivial. For large open wounds, injectable PEG–PPS hydrogels have however been shown to reduce neutrophil recruitment and enhanced wound closure.[27] More recently, thioether-functionalized hyaluronic acid was electrospun into nanofibres and formed fast-resorbing hydrogels that were highly antioxidant, anti-inflammatory, and significantly promoted wound closure/healing in a diabetic wound model.[28] These data lend support for the expanded use of polysulfides/PPS as anti-inflammatory agents in topical wound-healing applications. However, slow-degrading crosslinked hydrogels and nanoparticle dispersions are not ideal for inflammatory skin disorders with a more diffuse skin coverage, such as chronic wounds (*e.g.* diabetic ulcers), psoriasis, and atopic dermatitis.

Previous studies have shown that polymeric nanoparticles can be encapsulated within polymeric electrospun fibres.[29–31] Herein, we report the electrospinning of PPS-nanoparticles (PPS-NPs) within the matrix of PEO fibres, with this process summarized in Scheme 1. Using a PEGylated surfactant (Pluronic F127), we first polymerized propylene sulfide from a dithiol initiator *via* miniemulsion polymerization; these PPS-nanodroplets were then crosslinked *in situ* using a tetrafunctional acrylate to provide PEGylated PPS-NPs. Crosslinked PEGylated PPS-NPs were selected as (i) crosslinking provides

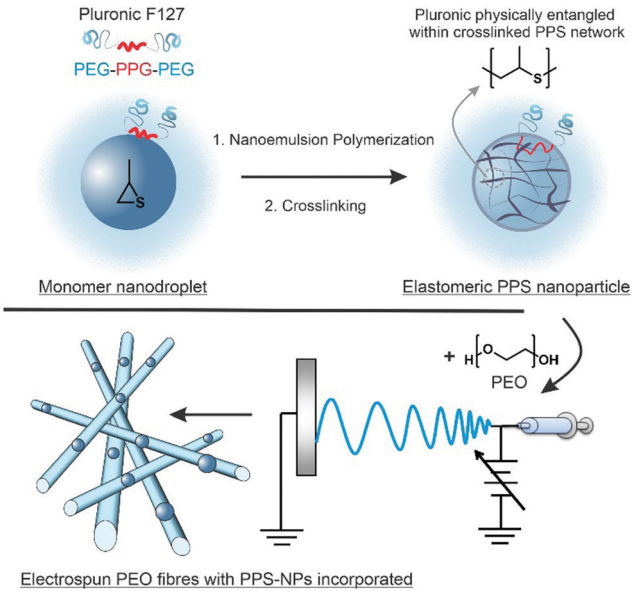

Scheme 1 Summary of PPS-NP polymerization and subsequent encapsulation into PEO fibres *via* electrospinning. Top: PPS-NPs (structure top right) are synthesized *via* a nanoemulsion polymerization utilizing as a droplet stabiliser the PEGylated surfactant Pluronic F127 which contains a poly(propylene glycol) (PPG) hydrophobic core-block. Bottom: PPS-NPs and PEO were electrospun from an aqueous solution into a sheet of nanofibres.

the chemical stability required for electrospinning, (ii) previous studies have demonstrated that Pluronic F127, loaded with anti-inflammatory lavender essential oils, readily encapsulates into PEO fibres *via* electrospinning[32] and (iii) PPS-NPs are extremely non-toxic, and potently antioxidant and anti-inflammatory.[16,23] PEO was selected as the polymer matrix as it is suited to controlling the dispersion of nanoparticles and fibre stability.[33] Furthermore, PEO has been found to promote wound-healing, likely due to its hygroscopic nature;[34] this is an important property for skin conditions characterized as a 'dry' wound such as atopic dermatitis and psoriasis. It should be noted that on wet wounds, PEO is known to dissolve relatively quickly;[35] however, to the best of our knowledge, PEO has not been evaluated in dry skin disorders. We predict that PEO will provide a significantly slower dissolution/resorption on dry wounds yielding a desirable sustained release profile, as well as creating a protective moisturizing layer that will promote healing.

2 Experimental

Materials

1,8-Diazabicyclo[5.4.0]undec-7-ene (DBU), 2,2′-(ethylenedioxy)-diethanethiol, lipopolysaccharides (LPS) (from *Escherichia coli* 0111:B4), poly(ethylene oxide) (PEO) with a viscosity average molecular weight (M_v) of 600 000 Da, propylene sulfide, pentaerythritol tetraacrylate, and Pluronic F127 were purchased from Sigma-Aldrich (Gillingham, UK) and used as received, besides pentaerythritol tetraacrylate which was first purified *via* column chromatography to give a crystalline solid.

Nanoparticle synthesis

PPS-NPs were prepared in a similar manner described by Jeanmaire *et al.* with minor adjustments.[16] Briefly, 15 mg of Pluronic F127 was dissolved in 20 mL of degassed MilliQ water within a Radley's 12-position carousel reaction vessel under an argon atmosphere. A stir speed of 850 rpm was set and 16.4 mg of 2,2′-(ethylenedioxy)diethanethiol (0.090 mmol) and 600 mg of propylene sulfide (8.093 mmol, corresponding to 45 equiv. per thiol) were added under a positive pressure argon flow. The mixture was allowed to stir for 10 min before 27.4 mg of DBU (0.180 mmol, 1 equiv. per thiol) was introduced to initiate the polymerization and the mixture was allowed 3.5 h to polymerize. The pH was then lowered to pH 8 by the addition of phosphate-buffered saline (PBS) salt (to make 50 mM solution) and a few drops of acetic acid, then 12.7 mg of the tetrafunctional crosslinker pentaerythritol tetraacrylate (0.036 mmol, 0.2 equiv. per thiol) dissolved in 0.1 mL of tetrahydrofuran (THF) was added to the reaction mixture. After 1 h, a further 6.3 mg of pentaerythritol tetraacrylate (0.018 mmol, 0.1 equiv. per thiol) was added in 0.1 mL of THF; immediately after the second addition of crosslinker, the pH was lowered to 7.4 with 0.1 M HCl and mixture was allowed to react under argon for an additional 16 h. Upon completion, the mixture was directly transferred to a Spectra-Por® Float-A-Lyzer with a MWCO of 100 kDa and dialyzed against MilliQ water for 5 days (water changed periodically each day). PPS-NPs were then filtered through a 0.45 μm PES filter and stored in the fridge until further use. The concentration of PPS-NPs was determined gravimetrically after sample lyophilization.

Electrospinning procedure

An aqueous suspension of PPS nanoparticles (1 wt%) was used and diluted to the concentrations seen in Table 1. PEO was then added to the six suspensions while stirring at 1000 rpm until they contained 7 wt% of polymer in total. The fibre loading concentration of PPS-NPs ranged from 1.0–14.3 wt% (deriving from a 0.7–10.0 mg mL^{-1} solution of PPS-NPs, respectively).

The solutions were then placed into the electrospinning setup comprising of a 40 kV DC power supply from Linari Engineering, a NE-300 syringe pump from New Era Pump Systems, and a grounded collector from Linari Engineering. The polymer solutions were loaded into a 1 mL syringe with a 21 gauge needle (inner diameter = 0.514 mm). All electrospinning experiments were conducted under the following conditions: 18 kV applied voltage, 0.5 mL h^{-1} flow rate, 12 cm working distance, and ambient environmental conditions.

Table 1 Composition of the six aqueous electrospinning solutions and PPS-NP concentration of the associated fibres

PEO (wt%)	PPS-NP (wt%)	Fibre PPS-NP conc. (wt%)
6.93	0.07	1.0
6.86	0.14	2.0
6.79	0.21	3.0
6.72	0.28	4.0
6.50	0.50	7.2
6.00	1.00	14.3

Electrospun fibre analysis

Scanning Electron Microscopy (SEM) was performed using a JEOL 7800F. The fibre diameter distribution was measured using the ImageJ plugin, DiameterJ, with a minimum of 7252 fibre diameter measurements per group. Energy-dispersive X-ray spectroscopy (EDS) was conducted on a JEOL 7800F. Point spectra were taken with the carbon, oxygen, and sulfur peaks being recorded. Dynamic Light Scattering (DLS) was conducted on an Anton Paar Litesizer 500.

Before SEM and EDS analysis, sections of the electrospun deposit, no more than 0.8 cm^2, were cut and attached to SEM sample stubs using a carbon adhesive tab and sputter coated in gold/palladium with a deposition current of 20 mA and tooling factor of 2.3 for 60 seconds.

Cells and cell culture

Human dermal fibroblasts (neonatal) (HDFn) were obtained from Thermo Fisher Scientific and used for cell viability assays; RAW264.7 macrophages were purchased from ATCC and used for cytokine stimulation experiments. Cells were cultured in Dulbecco's Modified Eagle Medium (DMEM) supplemented with 10% v/v fetal bovine serum, 2 mM L-glutamine, penicillin (100 U mL^{-1}), and streptomycin (0.1 mg mL^{-1}) at 37 °C in a humidified 5% CO_2 atmosphere.

Cytotoxicity

The cell viability of PPS-NPs and PPS-NP-loaded fibres were assessed in HDFn cells *via* the MTS assay. 10^4 HDFn cells were seeded into each well of a 96-well plate and allowed to adhere for 24 h in DMEM complete medium. Media was then exchanged for 100 μL of fresh media containing 0.001, 0.010, 0.050, 0.100, 0.500, 0.750, 1.000, and 2.000 mg mL^{-1} of PPS-NPs. Fibres containing 7.2 or 14.3 wt% of PPS-NPs were directly dissolved into the fresh media at targeted PPS-NP concentration. After 24 or 48 h of exposure, media was discarded, cells were rinsed with PBS, and 120 μL of MTS solution (Cell Titer 96 Aqueous One Solution Reagent in medium prepared following the manufacturer instructions) was added to each well and the plate was incubated for 1 h at 37 °C. MTS absorbance at 490 nm was measured and represented as a percentage of untreated controls.

Anti-inflammatory effect of PPS-NPs (TNF-α inhibition)

RAW264.7 macrophages were seeded in wells of a 24-well plate at a density of 1.5×10^5 cells per well and allowed to adhere in DMEM complete medium. After 24 h, media was removed and exchanged with fresh media containing 50 ng mL^{-1} LPS and 0, 0.10, 0.25, 0.50 or 1.00 mg mL^{-1} of PPS-NPs (*i.e.* by direct dissolution of fibres into the media). After a further 24 h the media was collected and analysed *via* a sandwich ELISA using the ThermoFisher Mouse TNFα ELISA (Enzyme-Linked Immunosorbent Assay) kit according to the manufacture's instruction.

3 Results & discussion

PPS-NPs were first synthesized from propylene sulfide monomer *via* a nanoemulsion polymerization before being electrospun into PEO fibres from aqueous solutions. The SEM micrographs of electrospun PEO fibres containing 0–14.3 wt% PPS-NPs in Fig. 1A–D show that homogenous fibres with narrow fibre diameter distributions were produced at these loading concentrations. The fibre diameter histogram seen in Fig. 1E shows that fibre diameter distributions are all monomodal with a median peak diameter between 150–204 nm. A slight increase in mean fibre diameter was observed as PPS-NPs were incorporated into the fibres, from an original diameter of 166 ± 19 nm (no PPS-NPs) to 191 ± 39 nm when loaded with 14.3 wt% PPS-NPs (Fig. 1F). This increase may be explained by the particles displacing their volume of the PEO matrix as they are encapsulated into the fibres. The increase in average fibre diameter is statistically significant at each loading concentration.

Although average fibre diameters increased significantly compared to the unloaded PEO fibres, fibres with low loading levels of PPS-NPs (Fig. 1B and C), do not present deformities indicative of nanoparticle encapsulation. Elsewhere, electrospun nanofibers portrayed significant irregularities due to an

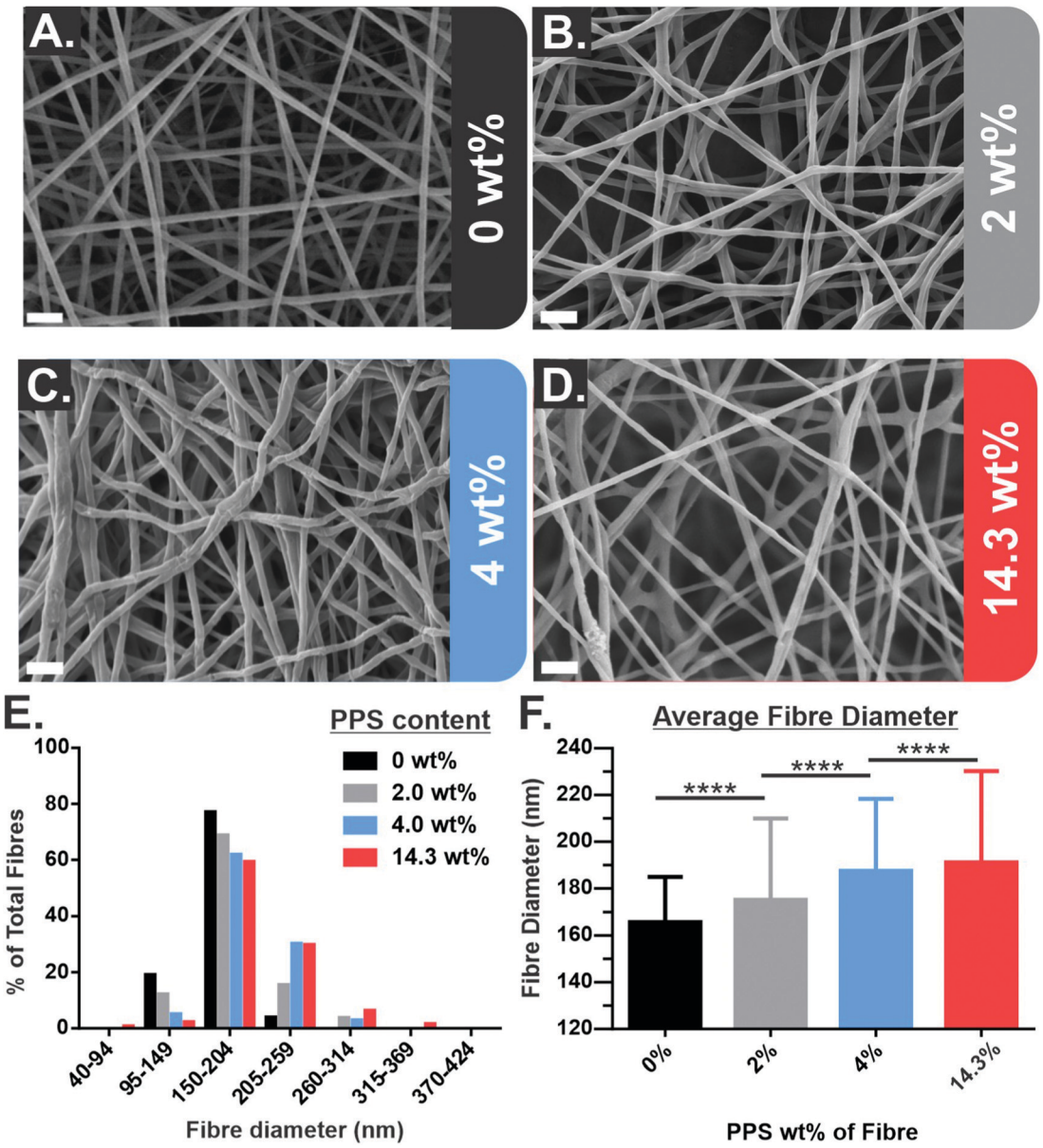

Fig. 1 SEM micrographs of the electrospun fibres containing 0, 2, 4, and 14.3 wt% (A, B, C and D respectively, scale bars = 1 μm) of PPS NPs, and corresponding fibre diameter histograms showing the fibre diameter distribution (E) and average fibre diameter (F). A two-way ANOVA followed by a Bonferroni *post hoc* analysis was used to compare statistical significance of mean diameters ($n > 7000$, ****; $p > 0.0001$, error bars = standard deviation).

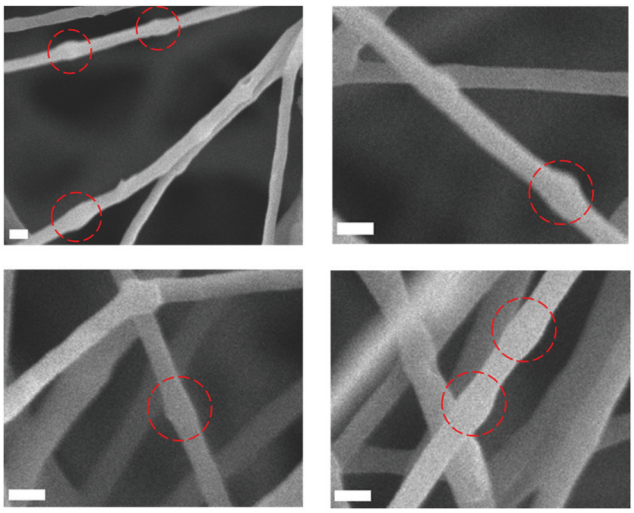

Fig. 2 SEM micrographs of electrospun PEO fibres containing ~14 wt% PPS-NPs displaying local diameter variations correlating to PPS-NP size (circled). Scale bars 250 nm.

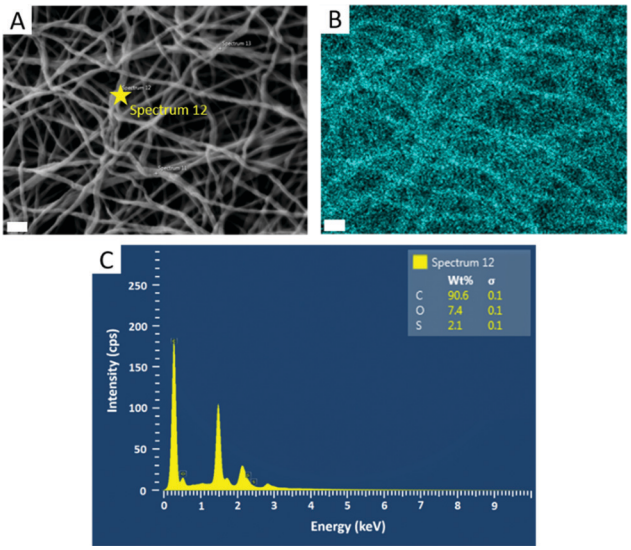

Fig. 3 Micrograph of PEO fibres containing 4 wt% PPS-NPs (A); EDS sulfur map of the same PEO fibres containing 4 wt% PPS-NPs (cyan = sulfur) (B); EDS point spectra taken from the fibre (C = carbon, O = oxygen, S = sulfur) (C). Scale bars 1 μm.

inhomogeneous distribution of nanoparticles,[36] or due to larger particle diameters which create more obvious deformities.[37] Since the PPS-NPs are coated in a PEGylated surfactant, Pluronic-F127, and the fibres themselves are composed of PEO (the same repeat unit as PEG), there is likely to be excellent compatibility and mixing between the two, which increases the likelihood of homogenous particle-in-fibre encapsulation.[31,33] At higher NP loadings (~14 wt%), potential nanoparticle-in-fibre deformities do present themselves (Fig. 1D).

These high-loading fibres were further analysed by SEM to better visualize potential particle encapsulation. Local fibre diameter variations/swellings could be observed in SEM micrographs (Fig. 2) and appear to correspond to the size of the PPS-NPs (Fig. 4). The locations highlighted in Fig. 2 (red circles) may contain PPS-NPs with diameters at the larger end of the particle size distribution, causing infrequent size variations ('bumps') in the local fibre diameter. This contrasts to PEO only fibres electrospun under the same conditions (shown in Fig. S1, ESI†) which contained almost no local diameter variations.

Further confirmation of particle encapsulation was found using EDS. From the sulfur map produced (Fig. 3), the sulfur content (Fig. 3B; cyan) is seen to overlap with the fibres in the associated SEM micrograph of fibres containing 4 wt% PPS-NPs (Fig. 3A). This contrasts with the sulfur map produced when observing PEO-only fibres without PPS-NPs (Fig. S2, ESI†) where no sulfur (cyan) could be detected. As the PPS-NP concentration within the blend was increased, the quantity of sulfur detected by EDS also increased confirming that PPS remains within the fibres after electrospinning; Table 2 displays the sulfur values recorded using EDS and the theoretical value calculated from the atomic masses and quantities of carbon, oxygen, and sulfur present in the fibres. To confirm that the particles remained intact after the electrospinning process, DLS was used to compare NP size before and after electrospinning (Fig. 4). Pristine PPS-NPs presented a monomodal size distribution with

Table 2 Comparison between expected sulfur content and observed sulfur content using EDS

PPS-NP concentration in fibres (wt%)	Theoretical sulfur content in fibre (wt%)	Observed sulfur content fibre (wt%)
1	0.4	0.7
2	0.8	0.8
3	1.2	1.5
4	1.6	2.1

a *Z*-ave. size of ~150 nm. Electrospun PPS-NP/PEO fibres were dissolved in water and re-evaluated by DLS; an almost identical

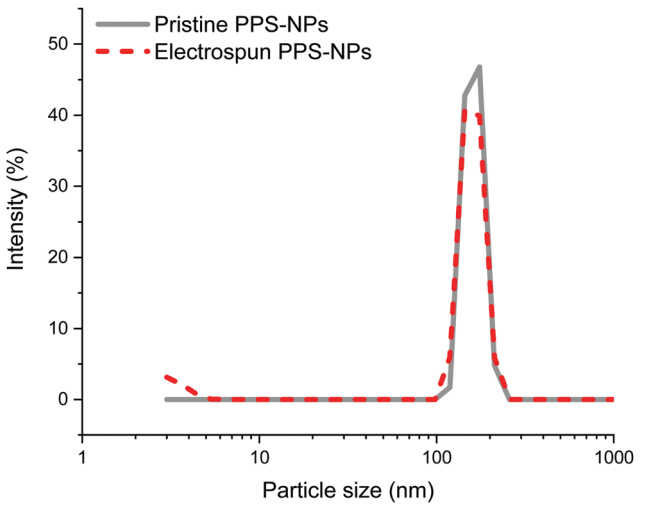

Fig. 4 Particle size distribution of pristine PPS nanoparticles (solid line) and resolubilized PEO/PPS-NP fibres (dashed line) indicating that the nanoparticles retained their size and morphology after electrospinning.

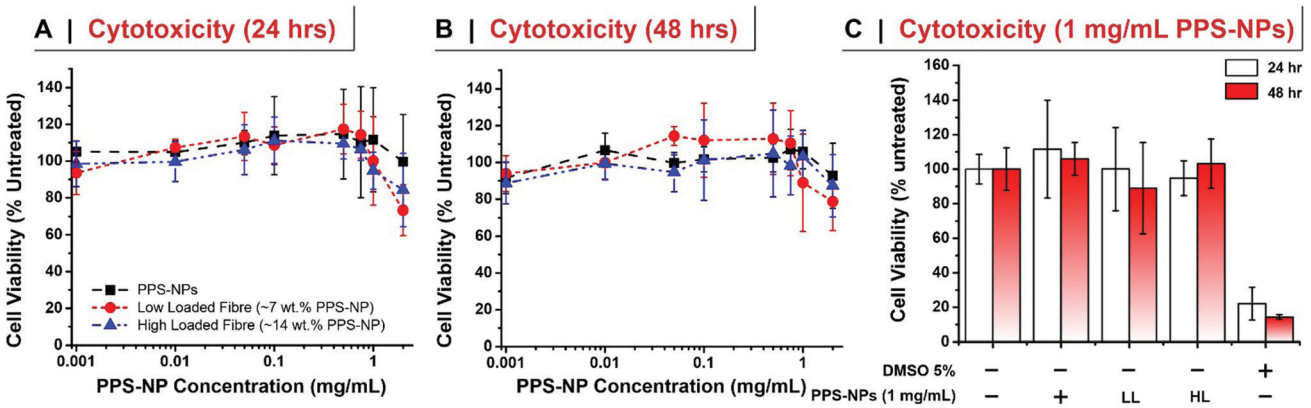

Fig. 5 The MTS assay was used to determine the cytotoxicity of PPS-NPs and PPS-NP-loaded fibres in HDFn cells at (A) 24 and (B) 48 h of exposure (n = 3). (C) Summary of HDFn cell viability exposed to 1 mg mL^{-1} of PPS-NPs either in solution or released from fibres containing a low-loading (LL) or high-loading (HL) of PPS-NPs (7.2 or 14.3 wt%, respectively). DMSO 5% is also displayed as a positive control.

distribution and Z-ave. size was measured indicating that the particles were encapsulated within the fibres in an unadulterated fashion and were thus unaffected by the electrospinning process.

DLS size distributions of the original PPS-NPs, electrospinning solution containing 0.7 wt% PEO and 0.1 wt% PPS-NPs, and the resolubilized fibres with their associated autocorrelation functions are shown in Fig. S3–S5 (ESI†). These results confirm that there is no change in particle size when blended with PEO as well as no change after electrospinning. It should be noted that after mixing PEO (before electrospinning) with PPS-NPs, a second PEO peak at ~5 nm is subsequently detected (Fig. S4, ESI†) and remains after resolubilization (Fig. 4 and Fig. S5, ESI†).

We further confirmed that after electrospinning the PPS-NPs retained their exceedingly low level of cytotoxicity in human dermal fibroblasts (HDFs) after 24 and 48 h of exposure (Fig. 5). At high concentrations of PPS-NPs (2 mg mL^{-1}) a slight reduction in cell viability was however observed with the electrospun nanoparticles (drop to ~80% viability); although not significantly different, this was less evident in the (non-spun) PPS-NPs. Interestingly, no significant difference was noted between the high loaded (14.3 wt% PPS-NP) and low loaded (7 wt%) fibres (Fig. 5C), this is despite the latter containing twice as much PEO mass per mg of PPS-NP. This confirms the biocompatibility of PEO, even at the high concentrations used, further justifying its use as fibre material. Overall, the PPS-NP-loaded fibres presented very little cytotoxicity, even as a highly concentrated solution, thus indicating their potential utility for skin-patch applications.

In recent works, PPS-NPs have demonstrated potent stand-alone anti-inflammatory and anti-stroke properties.[23] To confirm that the particles retain their anti-inflammatory nature after electrospinning, an ELISA was conducted to measure TNF-α levels in LPS-stimulated RAW264.7 macrophages. When RAW264.7 macrophages are stimulated with LPS, the inflammatory response results in the increased synthesis of inflammatory cytokines such as TNF-α.

Previous reports have demonstrated the ability of PPS-NPs to ameliorate production of TNF-α and interleukin-6 (IL-6) inflammatory cytokines in LPS-stimulated BV2 microglial cells and primary mixed glial cells.[23] These potent anti-inflammatory effects likely stem from the antioxidant nature of the polysulfide core. Here we demonstrate that their anti-inflammatory properties also transfer to LPS stimulated RAW264.7 macrophages. PPS-NP/PEO fibres were directly solubilized into the cell culture media as we believe this best replicates the 'released' state of the PPS-NPs expected to occur on the skin (PEO fibres were typically solubilized within minutes of addition to media). The PPS-NPs released from electrospun fibres retained their potent anti-inflammatory properties with a reduction to near baseline (no LPS stimulation) TNF-α levels when exposed to only 0.5 mg mL^{-1} of PPS-NPs (Fig. 6).

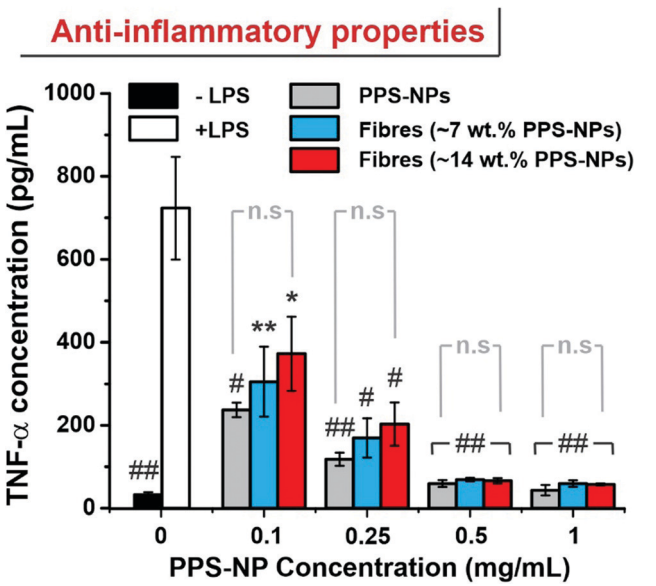

Fig. 6 The anti-inflammatory character of PPS-NPs was evaluated using TNF-α levels from LPS-stimulated RAW264.7 macrophages. Stimulated macrophages were exposed to PPS-NPs or fibres containing PPS-NPs at concentrations 0–1 mg mL^{-1} for 24 h (LPS controls, n = 6, treatment groups, n = 3). A two-way ANOVA followed by a Dunnett's tests were used to compare statistical significance to the +LPS control or a Šidák method to compare between treatment means (n.s.; $p > 0.05$, *; $p \leq 0.05$, **; $p \leq 0.01$, #; $p \leq 0.001$, ##; $p \leq 0.0001$).

Although the unspun PPS-NPs trended a slightly lower mean TNF-α concentration when dose matched to PPS-NP concentration, this was not significantly different to TNF-α concentrations of electrospun PPS-NPs, indicating the viability of electrospinning PPS-NPs whilst maintaining functionality upon their release. Previous studies on partially oxidized PPS, poly(propylene sulfoxide) (PPSO), have also demonstrated anti-inflammatory behaviour in LPS stimulated RAW264.7 macrophages,[38] albeit, less potently than PPS here. This likely stems from the slower oxidation of sulfoxides to sulfones and the lower oxidation capacity with respect to sulfides (first to sulfoxides, then to sulfones). This study also confirmed that in response to LPS stimulation, RAW264.7 macrophages produce high levels of H_2O_2 and hypochlorite which can be effectively scavenged by polymeric antioxidants. This is important as oxidants act as secondary messengers which, if left unattenuated, activate inflammatory pathways/signalling (*i.e.* NF-kB) and stimulate downstream TNF-α synthesis.[39,40]

The reduction in TNF-α, an M1 macrophage phenotype marker, may correspond to a phenotype reversal or shifting of an M1 (inflammatory) phenotype to an M2 (anti-inflammatory) phenotype. Indeed, recent studies on polysulfide hydrogels used in a diabetic wound found that ROS scavenging promoted an M1 to M2 transition and subsequently accelerated wound-healing and tissue remodelling.[28]

In the context of a topical patch for *e.g.* psoriasis, a sustained release of payload and full resorption of scaffold/fibre mesh are desirable outcomes. Herein, we have successfully demonstrated the synthesis and production of an antioxidant and anti-inflammatory resorbable fibrous patch with the potential to treat inflammatory skin disorders characterized by a dry/low-exudate topology. Future works will look to evaluate this system in appropriate animal models as well as to modulate scaffold dissolution properties (*e.g. via* crosslinking) to expand their functionality to 'wetter'/higher exudate skin wounds/disorders.

4 Conclusions

Homogenous, electrospun nanofibers with a narrow fibre diameter distribution were produced from aqueous solutions of PEO & PPS nanoparticles. SEM of nanofibres containing a high wt% loading of PPS-NPs suggested that particles had been fully encapsulated with great compatibility in the PEO fibres. EDS further confirmed that the PPS-NPs were incorporated into the electrospun PEO fibres and DLS after fibre dissolution confirmed that the nanoparticles retained their size and morphology after electrospinning. An ELISA for TNF-α further confirmed that the PPS-NPs also retained their antioxidant/anti-inflammatory nature after electrospinning. This system represents one of the few examples of (soft) organic nanoparticle encapsulation through electrospinning. We further believe this system represents a highly promising nanoparticle-scaffold hybrid material that warrants further investigation for sustained release application of anti-inflammatory particles/payloads, particularly for inflammatory skin pathologies.

Conflicts of interest

There are no conflicts to declare.

Acknowledgements

The authors acknowledge use of the facilities and the assistance of Dr Keith Yendall in the Loughborough Materials Characterisation Centre.

References

1 T. D. Rachakonda, C. W. Schupp and A. W. Armstrong, Psoriasis prevalence among adults in the United States, *J. Am. Acad. Dermatol.*, 2014, **70**(3), 512–516.
2 J. I. Silverberg, J. M. Gelfand, D. J. Margolis, M. Boguniewicz, L. Fonacier and M. H. Grayson, *et al.*, Atopic Dermatitis in US Adults: From Population to Health Care Utilization, *J. Allergy Clin. Immunol.*, 2019, **7**(5), 1524–1532.e2.
3 G. Goldenberg, Optimizing Treatment Approaches in Seborrheic Dermatitis, *J. Clin. Aesthet. Dermatol.*, 2013, **6**, 44–49.
4 M. A. Gupta and A. K. Gupta, Psychiatric and Psychological Co-Morbidity in Patients with Dermatologic Disorders Epidemiology and Management, *Am. J. Clin. Dermatol.*, 2003, **4**, 833–842.
5 J. Kessel and G. Goldenberg, Therapies to Improve the Cosmetic Symptoms of Atopic Dermatitis, *Adv. Cosmet. Dermatol.*, 2016, 183–186.
6 D. H. Reneker and I. Chun, Nanometre diameter fibres of polymer, produced by electrospinning, *Nanotechnology*, 1996, **7**, 216–223.
7 C. Huang, S. Chen, C. Lai, D. H. Reneker, H. Qiu and Y. Ye, *et al.*, Electrospun polymer nanofibres with small diameters, *Nanotechnology*, 2006, **17**(6), 1558–1563.
8 M. R. MacEwan, S. MacEwan, T. R. Kovacs and J. Batts, What Makes the Optimal Wound Healing Material? A Review of Current Science and Introduction of a Synthetic Nanofabricated Wound Care Scaffold, *Cureus*, 2017, **9**(10), e1736.
9 D. Kossyvaki, G. Suarato, M. Summa, A. Gennari, N. Francini and I. Gounaki, *et al.*, Keratin–cinnamon essential oil biocomposite fibrous patches for skin burn care, *Mater. Adv.*, 2020, **1**(6), 1805–1816.
10 J. Zeng, A. Aigner, F. Czubayko, T. Kissel, J. H. Wendorff and A. Greiner, Poly(vinyl alcohol) nanofibers by electrospinning as a protein delivery system and the retardation of enzyme release by additional polymer coatings, *Biomacromolecules*, 2005, **6**(3), 1484–1488.
11 K. D. McKeon-Fischer and J. W. Freeman, Characterization of electrospun poly(L-lactide) and gold nanoparticle composite scaffolds for skeletal muscle tissue engineering, *J. Tissue Eng. Regener. Med.*, 2011, **5**(7), 560–568.
12 Z. Xie, C. B. Paras, H. Weng, P. Punnakitikashem, L. C. Su and K. Vu, *et al.*, Dual growth factor releasing multifunctional nanofibers for wound healing, *Acta Biomater.*, 2013, **9**(12), 9351–9359.

13 C. R. Dejulius, A. Bernardo-Colón, S. Naguib, J. R. Backstrom, T. Kavanaugh and M. Gupta, *et al.*, Microsphere antioxidant and sustained erythropoietin-R76E release functions cooperate to reduce traumatic optic neuropathy, *J. Controlled Release*, 2020, DOI: 10.1016/j.jconrel.2020.10.010.

14 C. D. Vo, G. Kilcher and N. Tirelli, Polymers and sulfur: what are organic polysulfides good for? Preparative strategies and biological applications, *Macromol. Rapid Commun.*, 2009, **30**, 299–315.

15 F. El-Mohtadi, R. d'Arcy and N. Tirelli, Oxidation-Responsive Materials: Biological Rationale, State of the Art, Multiple Responsiveness, and Open Issues, *Macromolecular Rapid Communications*, Wiley-VCH Verlag, 2019, vol. 40.

16 D. Jeanmaire, J. Laliturai, A. Almalik, P. Carampin, R. D'Arcy and E. Lallana, *et al.*, Chemical specificity in REDOX-responsive materials: the diverse effects of different Reactive Oxygen Species (ROS) on polysulfide nanoparticles, *Polym. Chem.*, 2014, **5**(4), 1393–1404.

17 P. Carampin, E. Lallana, J. Laliturai, S. C. Carroccio, C. Puglisi and N. Tirelli, Oxidant-dependent REDOX responsiveness of polysulfides, *Macromol. Chem. Phys.*, 2012, **213**(19), 2052–2061.

18 A. Napoli, M. Valentini, N. Tirelli, M. Müller and J. A. Hubbell, Oxidation-responsive polymeric vesicles, *Nat. Mater.*, 2004, **3**(3), 183–189.

19 C. Dunnill, T. Patton, J. Brennan, J. Barrett, M. Dryden and J. Cooke, *et al.*, Reactive oxygen species (ROS) and wound healing: the functional role of ROS and emerging ROS-modulating technologies for augmentation of the healing process, *Int. Wound J.*, 2017, **14**(1), 89–96.

20 I. Khmaladze, K. S. Nandakumar and R. Holmdahl, Reactive oxygen species in psoriasis and psoriasis arthritis: relevance to human disease, *Int. Arch. Allergy Immunol.*, 2015, **166**(2), 135–149.

21 N. Sivaranjani, S. Venkata Rao and G. Rajeev, Role of reactive oxygen species and antioxidants in atopic dermatitis, *J. Clin. Diagn. Res.*, 2013, **7**(12), 2683–2685.

22 D. Yoo, A. W. Magsam, A. M. Kelly, P. S. Stayton, F. M. Kievit and A. J. Convertine, Core-Cross-Linked Nanoparticles Reduce Neuroinflammation and Improve Outcome in a Mouse Model of Traumatic Brain Injury, *ACS Nano*, 2017, **11**(9), 8600–8611.

23 O. Rajkovic, C. Gourmel, R. d'Arcy, R. Wong, I. Rajkovic and N. Tirelli, *et al.*, Reactive Oxygen Species-Responsive Nanoparticles for the Treatment of Ischemic Stroke, *Adv. Ther.*, 2019, 1900038.

24 K. P. O'Grady, T. E. Kavanaugh, H. Cho, H. Ye, M. K. Gupta and M. C. Madonna, *et al.*, Drug-Free ROS Sponge Polymeric Microspheres Reduce Tissue Damage from Ischemic and Mechanical Injury, *ACS Biomater. Sci. Eng.*, 2018, **4**(4), 1251–1264.

25 J. Zhang, T. Tokatlian, J. Zhong, Q. K. T. Ng, M. Patterson and W. E. Lowry, *et al.*, Physically associated synthetic hydrogels with long-term covalent stabilization for cell culture and stem cell transplantation, *Adv. Mater.*, 2011, **23**(43), 5098–5103.

26 F. El Mohtadi, R. D'Arcy, J. Burke, J. M. Rios De La Rosa, A. Gennari and R. Marotta, *et al.*, ''Tandem'' Nanomedicine Approach against Osteoclastogenesis: Polysulfide Micelles Synergically Scavenge ROS and Release Rapamycin, *Biomacromolecules*, 2020, **21**(2), 305–318.

27 S. Zhu, S. Li, H. Escuin-Ordinas, R. Dimatteo, W. Xi and A. Ribas, *et al.*, Accelerated wound healing by injectable star poly(ethylene glycol)-*b*-poly(propylene sulfide) scaffolds loaded with poorly water-soluble drugs, *J. Controlled Release*, 2018, **282**, 156–165.

28 S. Liu, Q. Zhang, J. Yu, N. Shao, H. Lu and J. Guo, *et al.*, Absorbable Thioether Grafted Hyaluronic Acid Nanofibrous Hydrogel for Synergistic Modulation of Inflammation Microenvironment to Accelerate Chronic Diabetic Wound Healing, *Adv. Healthcare Mater.*, 2020, **9**, 11.

29 M. Beck-Broichsitter, M. Thieme, J. Nguyen, T. Schmehl, T. Gessler and W. Seeger, *et al.*, Novel ''Nano in Nano'' Composites for Sustained Drug Delivery: Biodegradable Nanoparticles Encapsulated into Nanofiber Non-Wovens, *Macromol. Biosci.*, 2010, **10**(12), 1527–1535.

30 I. S. Chronakis, A. Jakob, B. Hagström and L. Ye, Encapsulation and selective recognition of molecularly imprinted theophylline and 17β-estradiol nanoparticles within electrospun polymer nanofibers, *Langmuir*, 2006, **22**(21), 8960–8965.

31 E. Jo, S. Lee, K. T. Kim, Y. S. Won, H. S. Kim and E. C. Cho, *et al.*, Core-sheath nanofibers containing colloidal arrays in the core for programmable multi-agent delivery, *Adv. Mater.*, 2009, **21**(9), 968–972.

32 H. Hajiali, M. Summa, D. Russo, A. Armirotti, V. Brunetti and R. Bertorelli, *et al.*, Alginate-lavender nanofibers with antibacterial and anti-inflammatory activity to effectively promote burn healing, *J. Mater. Chem. B*, 2016, **4**(9), 1686–1695.

33 G. M. Kim, A. Wutzier, H. J. Radusch, G. H. Michler, P. Simon and R. A. Sperling, *et al.*, One-dimensional arrangement of gold nanoparticles by electrospinning, *Chem. Mater.*, 2005, **17**(20), 4949–4957.

34 F. Yoshii, Y. Zhanshan, K. Isobe, K. Shinozaki and K. Makuuchi, Electron beam crosslinked PEO and PEO/PVA hydrogels for wound dressing, *Radiat. Phys. Chem.*, 1999, **55**(2), 133–138.

35 F. Qu, M. P. Pintauro, J. E. Haughan, E. A. Henning, J. L. Esterhai and T. P. Schaer, *et al.*, Repair of dense connective tissues *via* biomaterial-mediated matrix reprogramming of the wound interface, *Biomaterials*, 2015, **39**, 85–94.

36 L. Ji, K. H. Jung, A. J. Medford and X. Zhang, Electrospun polyacrylonitrile fibers with dispersed Si nanoparticles and their electrochemical behaviors after carbonization, *J. Mater. Chem.*, 2009, **19**(28), 4992–4997.

37 J. M. Lim, J. H. Moon, G. R. Yi, C. J. Heo and S. M. Yang, Fabrication of one-dimensional colloidal assemblies from electrospun nanofibers, *Langmuir*, 2006, **22**(8), 3445–3449.

38 F. el Mohtadi, R. D'Arcy, X. Yang, Z. Y. Turhan, A. Alshamsan and N. Tirelli, Main chain polysulfoxides as active 'stealth' polymers with additional antioxidant and anti-inflammatory behaviour, *Int. J. Mol. Sci.*, 2019, **20**, 18.
39 C. Bubici, S. Papa, K. Dean and G. Franzoso, Mutual cross-talk between reactive oxygen species and nuclear factor-kappa B: molecular basis and biological significance, *Oncogene*, 2006, **25**, 6731–6748.
40 N. Nakao, T. Kurokawa, T. Nonami, G. Tumurkhuu, N. Koide and T. Yokochi, Hydrogen peroxide induces the production of tumor necrosis factor-α in RAW 264.7 macrophage cells via activation of p38 and stress-activated protein kinase, *Innate Immun.*, 2008, **14**(3), 190–196.